

# EXPERIMENTAL STUDY OF FREE CONVECTION HEAT TRANSFER IN THE POROUS METAL-FOAM HEAT SINK

Tzer-Ming Jeng, Sheng-Chung Tzeng and Zhi-Ting Yeh  
Department of Mechanical Engineering, Chienkuo Technology University, Changhua County, 500, Taiwan  
E-mail: tmjeng@cc.ctu.edu.tw; tsc@ctu.edu.tw; lift6542@yahoo.com.tw

ICETI 2012-J1173\_SCI  
No. 13-CSME-75, E.I.C. Accession 3533

---

## ABSTRACT

This study experimentally investigated the free convection heat transfer characteristics of the annular metal-foam heat sinks. The results showed that the heat transfer coefficient ( $h$ ) decreased as the pore density of metal foams increased when the thickness ( $t_c$ ) of the annular metal foams equaled 5 mm, but the ( $h$ ) increased as the pore density increased when  $t_c = 11$  and 14.5 mm. Besides, the ( $h$ ) increased firstly and then decreased as ( $t_c$ ) increased. There was better heat transfer effect when  $t_c = 11$  mm in the present study.

**Keywords:** free convection heat transfer; metal-foam heat sink; experiment.

---

## ÉTUDES EXPÉRIMENTALES SUR LE TRANSFERT D'ÉNERGIE EN CONVECTION LIBRE DANS UN Puits THERMIQUE EN MOUSSE MÉTALLIQUE POREUSE

### RÉSUMÉ

Cette recherche expérimente les caractéristiques de transfert d'énergie en convection libre dans l'espace annulaire d'un puits thermique en mousse métallique poreuse. Les résultats montrent que le coefficient ( $h$ ) de transfert d'énergie diminue pendant que la densité poreuse de la mousse métallique augmente quand l'épaisseur ( $t_c$ ) de la mousse métallique dans l'espace annulaire est égale à 5 mm, mais que ( $h$ ) augmente quand la densité poreuse augmente quand  $t_c = 11$  et 14.5 mm. De plus ( $h$ ) commence par augmenter, et diminue quand ( $t_c$ ) augmente. On a constaté dans l'étude un meilleur effet de transfert d'énergie quand  $t_c = 11$ .

**Mots-clés :** transfert d'énergie en convection libre ; puits thermique en mousse métallique ; expérience.

## NOMENCLATURE

|                      |  |
|----------------------|--|
| $a_{sf}$             | heat-transfer area in unit volume of metal-foam material ( $\text{m}^2/\text{m}^3$ )   |
| $A$                  | area of bottom heated surface ( $\text{m}^2$ )   |
| $h$                  | heat transfer coefficient ( $\text{W}/\text{m}^2/\text{K}$ )   |
| $h_{sf}$             | natural convection heat transfer coefficient between the solid of metal foams and air ( $\text{W}/\text{m}^2/\text{K}$ )   |
| $H$                  | height of test specimen (m)  |
| $I$                  | input current (I)  |
| $Q_c$                | dissipated heat via natural convection from test specimen (W)  |
| $Q_{\text{LOSS}}$    | total heat loss (W)  |
| $Q_{\text{LOSS1}}$   | heat dissipated to the environment from the exposed part on both ends of heating foil (W)  |
| $Q_{\text{LOSS2}}$   | dissipated heat via natural convection from the bakelite block covered on the top of test specimen (W)   |
| $Q_{\text{LOSS3}}$   | dissipated heat via natural convection from the iron block pressed on the bakelite-block cover (W)   |
| $Q_{\text{LOSS4}}$   | heat loss at the bakelite base body at the bottom of test specimen (W)   |
| $Q_{\text{LOSS5}}$   | dissipated heat via natural convection from the iron bar supporting the bakelite-block cover (W)   |
| $Q_t$                | total input electric heat (W)  |
| $t_c$                | thickness of the annular copper-foam layer (m)   |
| $T$                  | temperature ( $^{\circ}\text{C}$ )   |
| $V$                  | input voltage (V)  |
| $V_{\text{foam}}$    | volume of metal-foam layer ( $\text{m}^3$ )  |
| <i>Greek symbols</i> |  |
| $\alpha$             | area ratio of stainless steel film heating foil in contacting with test specimen   |
| $\beta$              | ratio of dissipated heat via natural convection from test specimen to ( $Q_c + Q_{\text{LOSS2}} + Q_{\text{LOSS3}}$ ) or ( $Q_c + Q_{\text{LOSS2}} + Q_{\text{LOSS5}}$ ) |
| $\Delta T$           | temperature difference between the heated surface and the environment ( $^{\circ}\text{C}$ )   |
| <i>Subscripts</i>    |  |
| $s$                  | solid surface  |
| $w$                  | heated wall  |
| $\infty$             | ambient  |

## 1. INTRODUCTION

Over the past decade, the LED lighting fixture has formally entered into the lighting fixtures market dominated by incandescent lamp and fluorescent lamp. Although it has only 2% market share at present, LED is estimated to have 46% of the 4.4 billion USD worth of lighting fixtures market in the U.S. by 2020 [1]. As the LED power increases continuously, the cooling design of LED becomes an urgent issue. The cooling design of LED can be divided into active and passive types. The passive type does not require additional power components, and is highly reliable and energy saving. In general, about 90% of its heat [2] is transferred from the LED's base plate to the heat sink by thermal conduction, and then dissipated to the ambient by natural convection generated by the temperature difference between the high-temperature cooling fins of the heat sink and the ambient. It has more advanced space in such heat transfer mechanism.

Huang [3] used the corona wind generated by electrohydrodynamics (EHD) technology to enhance the convection effect of LED's cooling fins. The experimental results showed that the heat transfer coefficient increased to 1.6–3 times of that of natural convection in the experimental DC voltage range of 1–16 kV. The heat transfer enhancement was proportional to the strength of supply voltage. Hsiao [4] investigated the natural convection heat transfer of LEDs with various geometric-shape heat sinks in different rated electric powers, and used the digital thermocouple meter and infrared thermograph to record the single

point temperature of electrode and global temperature field of heat sink respectively. The heat sinks in four geometric shapes were set in the same surface area, which were plate fin, pin fin, staggered elliptical pin fin and staggered diamond shaped pin fin heat sinks. The experimental results showed that the staggered diamond shaped pin fin heat sink had more significant cooling effect on LED, followed by the staggered elliptical pin fin heat sink, and the pin fin heat sink. The plate fin heat sink had the worst cooling effect. Chiu [5] studied the heat transfer of LED, and extensively introduced the present heat transfer engineering technology for LED headlight of automobile. He discussed various heat transfer principles of LED headlight of automobile and the feasibility of application. Wu [6] combined semiconductor thermoelectric cooling module with cooling fin and fan for experiments. The experimental results showed that the semiconductor thermoelectric cooling module could cool down the LED's base plate by more than 10° C in the cooling state without fan. The effect was better when the fan was adopted. Hong [7] integrated the thermoelectric cooling module into finned heat sink for the cooling design of LEDs. He theoretically analyzed the heat transfer capability of such cooling device in the natural convection state, and found the optimal space between fins and base-plate thickness for the specified case. Chen [8] used experimental measurement and numerical simulation to explore the heat transfer performance of LED's cooling module. The results showed that the cooling area was enlarged but the heat transfer performance was not increased when the length of fins exceeded some critical value. The overall heat transfer capability of forced convection was 6–8 times high than that of natural convection. The numerical simulation results showed that the chimney effect in natural convection were helpful to heat transfer enhancement. Chen [9] used analytical simulation software to analyze the effect of geometric configuration of the base plate on heat transfer in the LED ceramic lamp. The results showed that the rise of LED junction temperature was related to the expansion of base-plate area, the base-plate thickness, and the thermal conductivity of material. Hong [10] used patent analysis to search for and analyze current heat transfer technologies used in high power LEDs, and used numerical method to investigate the heat transfer of LEDs. The simulation results showed that the cooling effect of thickening the fins was more obvious than that of enlarging the heat-transfer area. Guo [11] used commercial software to simulate the heat transfer of LEDs in different powers, and studied the heat transfer enhancement after the application of aluminum finned heat sink. The simulation results showed that the heat sink was obviously helpful to reducing the LED operating temperature. Most of the above studies on LED heat transfer were limited to investigating the cooling efficiency of traditional finned cooling module, and used numerical simulation method. In addition, Weng [12] and Hetsroni et al. [13] studied the natural convection heat transfer characteristics in porous medium, but did not use this novel material in the research on LED heat transfer.

This study proposed cooling LED by using metal foamed material instead of traditional cooling fins. In recent years, the porous medium material has been widely used in the heat transfer of electronic modules. It has two major advantages: first, porous medium material increases the surface area by tens of times for heat transfer, so that the heat is easier to dissipate; second, the irregular porous internal structure results in irregular motion of fluid that causes extra dissipated heat transfer capacity. Therefore, the heat transfer capability of porous medium material is much better than that of purely smooth surface. This study attempted to use experimental method to investigate the proper configuration design for the annular porous medium heat sink. The heat transfer capability of natural convection was estimated to be improved effectively. To the best of our knowledge, this design has never been published in previous works, thus, it has considerable values in research and practical application.

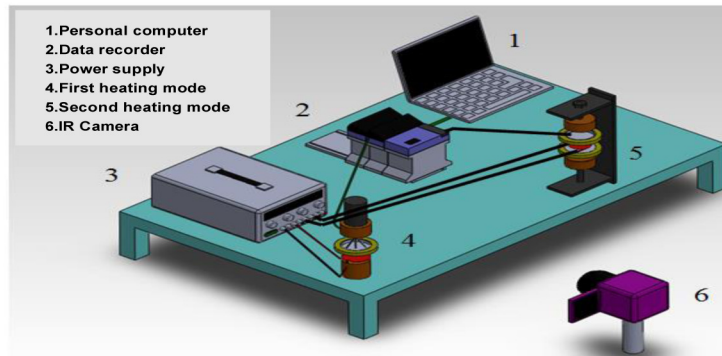


Fig. 1. Experimental equipments.

## 2. EXPERIMENT

### 2.1. Experimental Setup

This study replaced traditional cooling fins by metal foamed material. The metal foamed material has high permeability and cooling area as large as several times of traditional fins. With a proper configuration design, it can improve the heat transfer capacity. This study experimentally explored the natural convection heat transfer characteristics of annular metal foamed heat sink applied to the cooling of LEDs. The heat sink was made of annular dish-shaped aluminum alloy with a diameter of 76 mm, a height of 14.6 mm and a thickness of 3 mm, adhered with annular copper-foam layer. The copper foams having the same porosity of 0.97 with different PPIs (pores per inch) were used as test materials. Different heat fluxes were applied to the bottom of heat sink. The variable parameters included the temperature difference ( $\Delta T$ ) between heated surface and environment, the PPI and the thickness ( $t$ ) of annular copper-foam material. The parameters were studied systematically to determine their effects on natural convection heat transfer. The results could serve as an important basis for developing the metal porous medium heat sink into the high performance cooling system of LEDs.

The experimental equipments for steady-state heat transfer and infrared thermal image measurements are shown in Fig. 1. There were two systems, steady-state heat transfer measurement system and infrared thermal image measurement system. The heat transfer measurement system was designed as two heating modes. Figure 2 shows the side views of heating platforms for Mode 1 and Mode 2. Mode 1 was designed for heating one test specimen. A heater was made, and the body of heater was a circular cylinder (in height of 70 mm and diameter of 70 mm) made of bakelite. A heating foil (in diameter of 70 mm) was placed on the bakelite body, adhered to the test specimen by the high-conductivity thermal grease, covered with a cylindrical bakelite block (in height of 47 mm and diameter of 70 mm), and then pressed by an iron block. This heating mode required only one test specimen for experimental measurement, but the experimental heat loss was large. Therefore, Mode 2 was designed as bilateral heating. In this mode, both sides of the heating foil were separately adhered to two test specimens of the same configuration, and the contact surfaces were coated with high-conductivity thermal grease to reduce the contact thermal resistance. The openings on both sides of two test specimens were covered with bakelite blocks, and then held and tightly pressed by the assembly of springs and iron bars. Although this mode required two test specimens, it could minimize the heat loss. This study compared these two heating modes with the test case without metal foamed material to determine the empirical equation of heat loss of the first heating mode (Mode 1). It then used Mode 1 as the main testing method for experimental measurement. The heater body in Mode 1 was a circular cylinder (in height of 70 mm and diameter of 70 mm) made of bakelite. The bottom surface of the test specimen was drilled three circular flutes (as shown in Fig. 3). Each flute held a circular copper sheet with a diameter

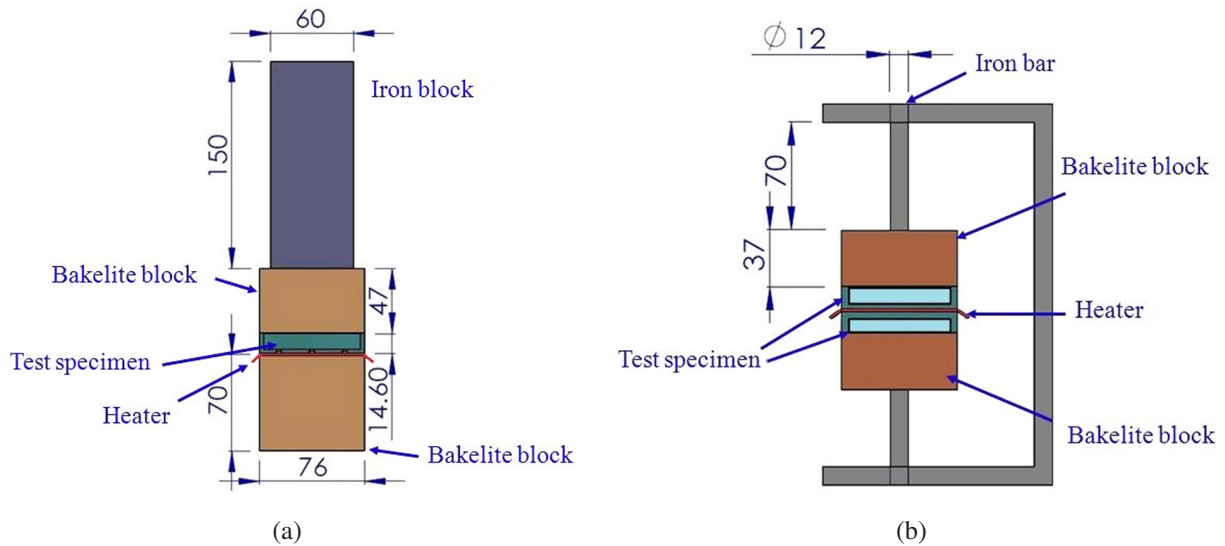


Fig. 2. Side views of the heating platforms (Unit: mm): (a) the first heating mode; (b) the second heating mode.

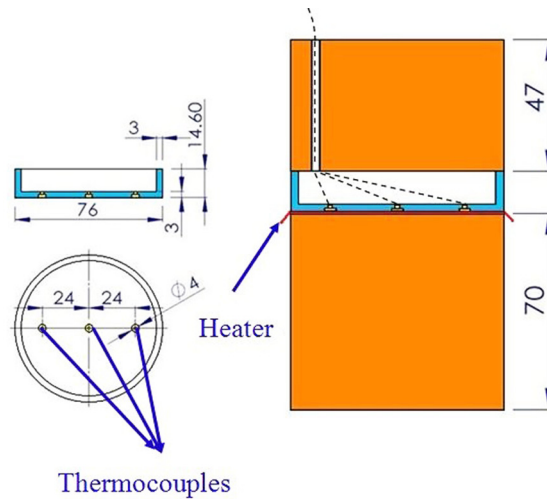


Fig. 3. Positions of thermocouples and heater (Unit: mm).

of 4 mm and a thickness of 1.5 mm. The balling end of the TT-T-30SLE T-type thermocouple was welded to the central part of copper sheet and the copper sheet was embedded in the flute of test specimen. The thermocouple wire penetrates through the bakelite body covered the opening of test specimen, and then was connected to the data recorder. The data recorder converted micro voltage variation data into temperature data, and stored the heated surface temperature in the computer. Two additional thermocouple wires were laid for monitoring the ambient temperature. Besides, both sides of the heating foil were coated with teflon films for insulation, so as to avoid the stainless steel film heating foil contacting the metal surface of test specimen directly to result in electric conduction. The heating foil was welded with power wire through the bakelite body, connected to the DC power supply. The DC power supply could regulate the voltage and current to control the electric heat fluxes.

This study used the hollow circular cylinder covered with metal foamed material. The metal hollow circular cylinder could transfer the heat by thermal conduction efficiently and the metal foamed material was for expanding the heat exchange area with the environment, resulting in a high performance heat transfer

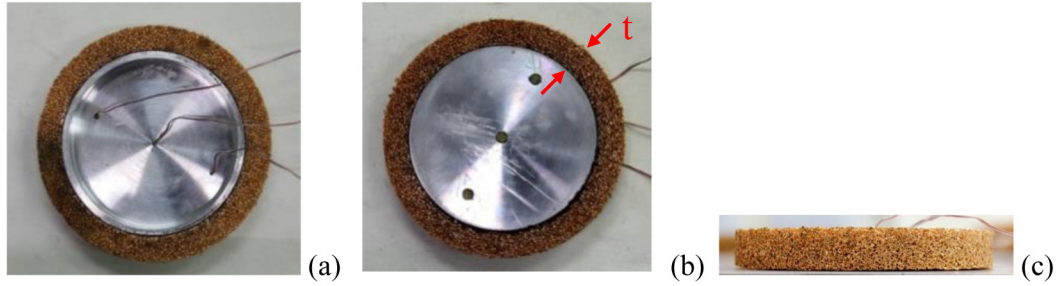


Fig. 4. Photos of the typical test specimen (Typical case:  $t = 11$  mm and  $\varepsilon = 0.97/30$  PPI): (a) top view; (b) bottom view; (c) side view.

path. The test specimen was made of annular dish-shaped aluminum alloy with a diameter of 76 mm, a height of 14.6 mm, and a thickness of 3 mm covered with annular metal foam layer in various thicknesses. The 0.97-porosity copper foams in different PPIs were used as the test materials. Different heat fluxes were applied to the bottom of test specimen. The variable parameters included the temperature difference ( $\Delta T$ ) between the heated surface and the environment, the PPI of copper foams and the thickness ( $t$ ) of annular copper foams. The ( $\Delta T$ ) was controlled at 30–60°C. The PPIs of the copper foams were 20, 30 and 40, respectively. The thicknesses ( $t$ ) of annular copper foams were 5, 11 and 14.5 mm, respectively. The test section is shown in Fig. 4.

## 2.2. Data Reduction and Uncertainty Analysis

### 2.2.1. Data reduction of the first heating mode (configuration without metal-foam layer)

$$\begin{aligned}
 Q_c &= Q_t - (Q_{\text{LOSS1}} + Q_{\text{LOSS2}} + Q_{\text{LOSS3}} + Q_{\text{LOSS4}}) \\
 &= Q_t - (1 - \alpha) \times Q_t - (1 - \beta) \times (Q_t - Q_{\text{LOSS1}} - Q_{\text{LOSS4}}) - Q_{\text{LOSS4}} \\
 &= \alpha\beta Q_t - \beta Q_{\text{LOSS4}}
 \end{aligned} \tag{1}$$

### 2.2.2. Data reduction of the second heating mode (configuration without metal-foam layer)

$$\begin{aligned}
 Q_c &= (Q_t - Q_{\text{LOSS1}})/2 - Q_{\text{LOSS2}} - Q_{\text{LOSS5}} \\
 &= (Q_t - Q_{\text{LOSS1}})/2 - (1 - \beta) \times (Q_t - Q_{\text{LOSS1}})/2 \\
 &= \alpha\beta Q_t/2
 \end{aligned} \tag{2}$$

where  $Q_c$  is the dissipated heat via natural convection from test specimen,  $Q_t$  is the total input electric heat,  $Q_{\text{LOSS1}}$  is the heat dissipated to the environment from the exposed part on both ends of heating foil,  $Q_{\text{LOSS2}}$  is the dissipated heat via natural convection from the bakelite block covered on the top of test specimen,  $Q_{\text{LOSS3}}$  is the dissipated heat via natural convection from the iron block pressed on the bakelite-block cover;  $Q_{\text{LOSS4}}$  is the heat loss at the bakelite base body at the bottom of test specimen; and  $Q_{\text{LOSS5}}$  is the dissipated heat via natural convection from the iron bar supporting the bakelite-block cover. As in the first heating mode,  $\alpha$  is the area ratio of stainless steel film heating foil in contacting with test specimen, while it is 0.87 in this experiment; and  $\beta$  is the ratio of dissipated heat via natural convection from test specimen to ( $Q_c + Q_{\text{LOSS2}} + Q_{\text{LOSS3}}$ ) for the first mode or ( $Q_c + Q_{\text{LOSS2}} + Q_{\text{LOSS5}}$ ) for the second mode. In general, the dissipated heat via natural convection from smooth plate surface can be expressed as in Eq. (3):

$$Q = h \cdot A \cdot (T_s - T_\infty) = C \cdot A \cdot (T_s - T_\infty)^{1.25} \tag{3}$$

where  $Q$  is dissipated heat,  $h$  is the heat transfer coefficient,  $A$  is the area of bottom heated surface,  $T_s$  is the temperature of solid surface; and  $T_\infty$  is the ambient temperature. Therefore,  $\beta = \text{test-specimen temperature difference}^{1.25} \times \text{test-specimen surrounding area} / [\text{test-specimen temperature difference}^{1.25} \times \text{test-specimen surrounding area} + \text{bakelite-block temperature difference}^{1.25} \times (\text{bakelite-block surrounding area} + \text{bakelite-block topside exposed area}) + \text{iron-block (or -bar) temperature difference}^{1.25} \times (\text{iron-block (or -bar) surrounding area} + \text{iron-block (or -bar) topside area})]$ .

### 2.2.3. Data reduction of the first heating mode (configuration with metal-foam layer)

$$Q_c = h \cdot A \cdot (T_W - T_\infty) \quad (4)$$

where  $Q_c$  is the dissipated heat via natural convection from test specimen,  $h$  is the heat transfer coefficient,  $A$  is the heated bottom area,  $T_W$  is the heated wall temperature; and  $T_\infty$  is the ambient temperature.

$$Q_c = h_{sf} \cdot (V_{\text{foam}} \cdot a_{sf}) \cdot (T_W - T_\infty) \quad (5)$$

where  $h_{sf}$  is the natural convection heat transfer coefficient between the solid of metal foams and air,  $V_{\text{foam}}$  is the volume of metal-foam layer; and  $a_{sf}$  is the heat-transfer area in unit volume of metal-foam material (specific area of metal-foam material).

$$Q_c = Q_t - Q_{\text{LOSS}} = I \cdot V - Q_{\text{LOSS}} \quad (6)$$

where  $Q_{\text{LOSS}}$  is the total heat loss,  $I$  is the input current; and  $V$  is the input voltage. The total heat loss  $Q_{\text{LOSS}}$  consists of four parts:

$$Q_{\text{LOSS}} = Q_{\text{LOSS1}} + Q_{\text{LOSS2}} + Q_{\text{LOSS3}} + Q_{\text{LOSS4}} \quad (7)$$

$Q_{\text{LOSS1}} = (1 - \alpha) \times Q_t$  and  $Q_{\text{LOSS2}}$ ,  $Q_{\text{LOSS3}}$  and  $Q_{\text{LOSS4}}$  are substituted in various empirical equations of heat loss obtained from Section 2.2.1 and 2.2.2 (see Fig. 5). Therefore:

$$Q_c = Q_t - (Q_{\text{LOSS1}} + Q_{\text{LOSS2}} + Q_{\text{LOSS3}} + Q_{\text{LOSS4}}) = \alpha Q_t - Q_{\text{LOSS2}} - Q_{\text{LOSS3}} - Q_{\text{LOSS4}} \quad (8)$$

The global error of experimental result includes the errors of measurement parameters and calculating parameters. The uncertainty of measurement parameters is resulted from the error of instrument system and the human reading error. The calculating parameters are formed from mutual calculation of measurement parameters. The uncertainty analysis of this experiment adopts Moffat [14] uncertainty analysis method. The uncertainties of heat transfer coefficient ( $h$ ) in this experiment is  $\pm 7.56\%$ .

## 3. RESULTS AND DISCUSSION

Figure 6 shows the relationship between heat transfer coefficient ( $h$ ) and  $\Delta T (= T_w - T_\infty)$  for various thicknesses of annular copper-foam layer ( $t_c = 5, 11, 14.5$  mm). It was observed that the heat transfer coefficient ( $h$ ) increased with  $\Delta T$ , meeting the natural convection heat transfer characteristics. It was because that the rise of  $\Delta T$  enhances the buoyancy effect and free convection, therefore increasing the heat transfer coefficient ( $h$ ).

In Fig. 6, when  $t_c = 5$  mm, the heat transfer coefficient ( $h$ ) decreased as the pore density (the value of PPI, pores per inch) of metal foams increased. However, when  $t_c = 11$  and 14.5 mm, the heat transfer coefficient ( $h$ ) increased as the pore density increased. It may be explained as follows. When PPI was small, the flow resistance was reduced, and the natural convection was likely to flow inside the metal foams, so the heat transfer coefficient ( $h$ ) increased. Second, when PPI was large, the specific area ( $a_{sf}$ ) of metal-foam material increased, and the total heat-exchange area increased, so the heat transfer coefficient ( $h$ ) increased. Obviously, when ( $t_c$ ) was very small (e.g.,  $t_c = 5$  mm), the former effect dominated heat transfer, whereas when ( $t_c$ ) was large (e.g.,  $t_c = 11$  and 14.5 mm), the latter effect dominated heat transfer.

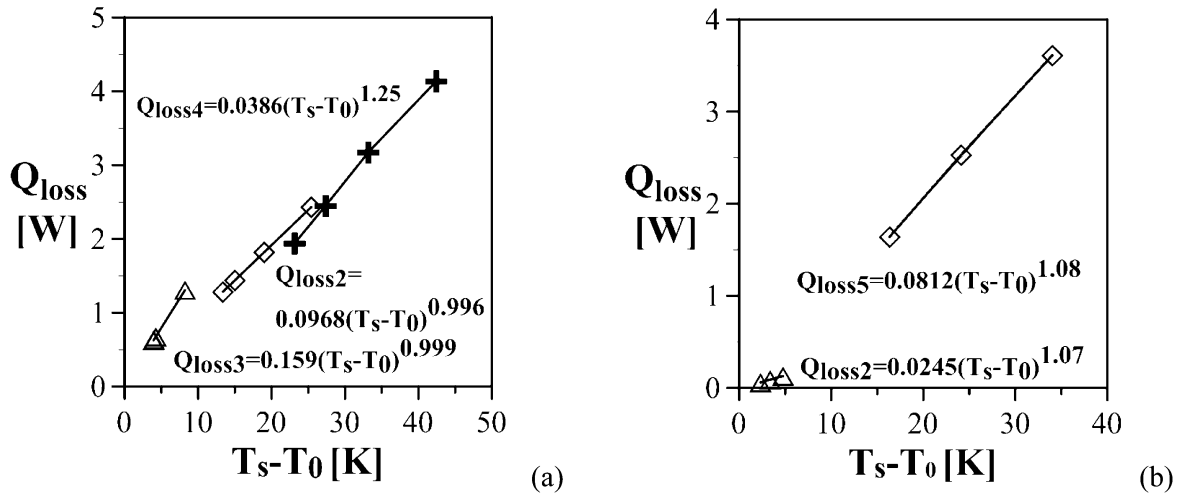


Fig. 5. Relationship between  $Q_{Loss}$  and  $\Delta T$ : (a) the first heating mode; (b) the second heating mode.

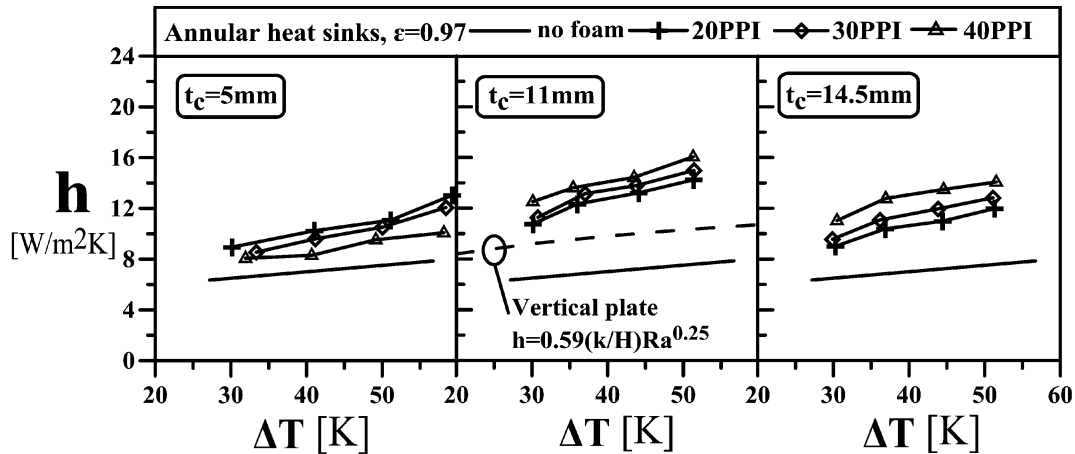


Fig. 6. Relationship between  $h$  and  $\Delta T$  for various  $t_c$ .

As far as the authors know, the free convection heat-transfer experiments for the annular metal foams are few. In order to validate the present experiments, the present data for the system without metal foams was compared with the previous free convection empirical result of the vertical plate reported by Holman [15].

$$h = 0.59(k/H)Ra^{0.25} \quad (9)$$

where  $h$  is the heat transfer coefficient of the nature convection from the vertical heated plate surface to the air,  $k$  is the thermal conductivity of air,  $H$  is the height of the test specimen and  $Ra$  is Rayleigh number based on  $H$ . As shown in Fig. 6, the trend of the present result for the pure metallic cup agrees with that predicted by Eq. (9). However, the present result is about 23% smaller than that predicted by Eq. (9). It should be induced by the temperature of the heated wall surface. The heated wall in Eq. (9) is the vertical plate; while the heated wall in the present test specimen is the bottom plate of the metallic cup. Therefore, Eq. (9) over predicts somewhat.

Figure 7 shows the relationship between heat transfer coefficient ( $h$ ) and thicknesses of annular copper-foam layer ( $t_c$ ) for different  $\Delta T$  and PPI. As seen, the heat transfer coefficient ( $h$ ) increased and then decreased as thickness ( $t_c$ ) increased. It was because that the total heat-transfer area expands as the thickness

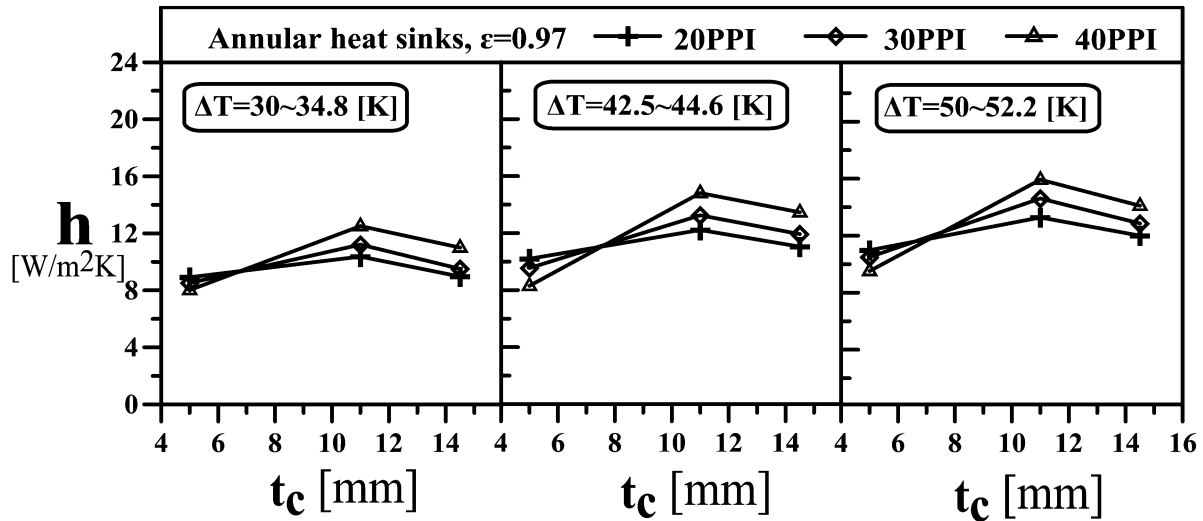


Fig. 7. Relationship between  $h$  and  $t$  for various  $\Delta T$ .

$(t_c)$  increases, which increases the heat transfer coefficient ( $h$ ). However, when the thickness ( $t_c$ ) increases continuously, the temperature difference between the external portion of annular metal-foam layer and the environment decreases due to the fin effect, so the heat transfer coefficient ( $h$ ) decreases. In addition, the reverse change of PPI effect discussed in Fig. 6 occurred at  $t_c = 6.5\text{--}7.5$  mm.

#### 4. CONCLUSIONS

This study experimentally investigated the free convection heat transfer characteristics of the annular metal foamed material, which was used to replace traditional cooling fins to form a high performance heat sink for LED lamp. The relevant variable parameters were the temperature difference ( $\Delta T = 30\text{--}50^\circ\text{C}$ ) between the heated wall and the ambient, the pore density (i.e. the value of pores per inch, PPI = 20–40) and the thickness ( $t_c = 5\text{--}14.5$  mm) of the annular metal foams. Major conclusions are summarized as follows:

1. The heat transfer coefficient ( $h$ ) increased with  $\Delta T$ .
2. When  $t = 5$  mm, the heat transfer coefficient ( $h$ ) decreased as PPI increased. However, when  $t_c = 11$  and 14.5 mm, the heat transfer coefficient ( $h$ ) increased with PPI. The reverse change of PPI effect occurred at  $t_c = 6.5\text{--}7.5$  mm.
3. The heat transfer coefficient ( $h$ ) increased firstly and then decreased as  $t_c$  increases from 5 to 14.5 mm. Among the test cases of this study, the test cases with  $t_c = 11$  mm and PPI = 40 had the best natural convection heat transfer capacity.

#### ACKNOWLEDGEMENTS

The authors would like to thank the National Science Council of the Republic of China for financially supporting this research under contract Nos. NSC 97-2221-E-344-003, NSC 99-2622-E-270-014-CC3, NSC 100-2221-E-270-014-MY3 and NSC 100-2632-E-270-001-MY3.

#### REFERENCES

1. Long, S., "Report: LED lights to capture 50 percent of market by 2020", *Electronics Cooling*, May 25th, 2010.

2. Petroski, J., "Thermal challenges in LED cooling", *Electronics Cooling*, Nov. 1st, 2006.
3. Huang, C.T., "Investigation of LED heat transfer enhancement by EHD technology", Master Thesis, Department of Power Mechanical Engineering at National Tsing Hua University, Taiwan, 2005.
4. Hsiao, C., "A study of LED's heat dissipation with different heat sinks", Master Thesis, Department of Mold and Die Engineering at National Kaohsiung University of Applied Sciences, Taiwan, 2007.
5. Chiu, K.H., "Study of light emitting diodes for the headlight illumination", Master Thesis, Department of Electronic Engineering at National Changhua University of Education, Taiwan, 2007.
6. Wu, J.C., "Study of LED heat transfer enhancement by thermoelectric cooling module", Master Thesis, Graduate Institute of Mechatronic System Engineering at National University of Tainan, Taiwan, 2007.
7. Hung, Y.C., "Investigation of LED cooling with thermoelectric cooler", Master Thesis, Department of Mechanical Engineering at National Taiwan University, Taiwan, 2007.
8. Chen, Z.D., "Experiment and numerical simulation on the flow and thermal fields of LED coolers", Master Thesis, Department of Mechanical and Mechatronic Engineering at National Taiwan Ocean University, Taiwan, 2008.
9. Chen, H.H., "A thermal analysis of substrate to high power LED in a ceramic lamp", Master Thesis, Department of Mechanical Engineering at Chung Yuan Christian University, Taiwan, 2008.
10. Shen, C.H., "A study on the patent analysis and numerically thermal simulation of high power LED", Master Thesis, Graduate School of Electric Engineering at Fortune Institute of Technology, Taiwan, 2008.
11. Kuo, B.C., "Thermal analysis of high power LEDs with advanced package", Master Thesis, Department and Graduate School of Electronic Engineering at Kao Yuan University, Taiwan, 2009.
12. Weng, L.C., "Heat transfer simulation of metal foam heat sink for LEDs", in *Proceedings of 18th CFD Conference*, Taiwan, August, 2011.
13. Hetsroni, G., Gurevich, M. and Rozenblit, R., "Natural convection in metal foam strips with internal heat generation", *Experimental Thermal and Fluid Science*, Vol. 32, pp. 1740–1747, 2008.
14. Moffat, R.J., "Contributions to the theory of single-sample uncertainty analysis", *ASME J. Fluids Engineering*, Vol. 104, pp. 250–260, 1986.
15. Holman, J.P., *Heat Transfer*, The McGraw-Hill Companies, Inc., New York, 1997.